POLITECNICO DI TORINO
Repository ISTITUZIONALE

Superconducting and hybrid magnetic shields: comparison between 3D modeling and experiment

Original
Superconducting and hybrid magnetic shields: comparison between 3D modeling and experiment / Gozzelino, L., Fracasso, M., Ferracin, S., Napolitano, A., Torsello, D.. - (2021). (7th International Workshop on Numerical Modelling of High Temperature Superconductors (HTS 2020)).

Availability:
This version is available at: 11583/2974765 since: 2023-01-18T11:14:56Z

Publisher:
Kévin Berger (Université de Lorraine - GREEN)

Published
DOI:

Terms of use:

This article is made available under terms and conditions as specified in the corresponding bibliographic description in the repository

Publisher copyright

(Article begins on next page)

27 November 2026

Superconducting and hybrid magnetic shields: comparison between 3D modeling and experiment

Laura Gozzelino
Politecnico di Torino, DISAT
Torino, Italy
laura.gozzelino@polito.it

Michela Fracasso
Politecnico di Torino, DISAT
Torino, Italy
michela.fracasso@polito.it

Samuele Ferracin
Politecnico di Torino, DISAT
Torino, Italy
samuele.ferracin@polito.it

Andrea Napolitano
Politecnico di Torino, DISAT
Torino, Italy
andrea.napolitano@polito.it

Daniele Torsello
Politecnico di Torino, DISAT
Torino, Italy
daniele.torsello@polito.it

***Abstract*— The use of superconducting (SC) materials is crucial for shielding quasi-static magnetic fields. However, a successful approach requires the availability of a modeling procedure that can be exploited to guide the shielding devices' design. In this work, we applied a 3D numerical modeling method based on the vector-potential formulation to predict the shielding properties of a short SC hollow cylinder with and without the superimposition of a ferromagnetic tube in both axial- and transverse-field configuration. Calculation outcomes were then compared with experimental data obtained on the same shielding arrangements. The agreement between computed and experimental results validates the simulation outputs and opens to the exploitation of this modeling approach for designing more efficient shielding solutions.**

Keywords— magnetic shielding, 3D numerical modeling, bulk superconductor

I. INTRODUCTION

Magnetic shielding is crucial for instruments requiring very low environmental magnetic field or to solve problems of electromagnetic compatibility among devices operating in the same location. For this purpose, the availability of numerical modeling techniques able to guide the shield design is fundamental in order to match practical requirements of both high shielding factors and space-saving solutions. In particular, shield design optimization under realistic working conditions requires a 3D modeling approach which allows the analysis of shielding properties for various orientations of the applied magnetic field [1].

Superconductors are key materials for shielding quasi-static magnetic fields [2]-[4]. Furthermore, improvements in their shielding performance have been proved by superimposing a sheet of ferromagnetic (FM) material [5]-[7]. However, also in this case, a 3D investigation is essential by reason of the non-trivial change of the shielding ability of a superconducting (SC) vessel with a small aspect ratio of height/radius when a FM vessel is superimposed [8].

In this work, we applied the numerical procedure based on the 3D magnetic vector-potential (**A**) formulation described in [9] to predict the shielding properties of a short SC hollow cylinder with and without the superimposition of a FM tube in both axial- and transverse-field configuration. To this aim, we considered a SC hollow cylinder with the same size and critical current density (J_c) dependence on magnetic induction field, B, as that studied in [10]. Computed B values were then compared with those measured experimentally by means of cryogenic Hall probes on the same shielding arrangements.

II. MODELING

Calculations were carried out by means of COMSOL Multiphysics® [11]. Following the numerical modeling procedure presented in [9], in order to reproduce the magnetic properties of the superconducting shield a hyperbolic tangent dependence of the current density, **J**, on the electric field, **E**, and, therefore on the time derivative of **A** was chosen. As in [9], we assumed that the local current density in the superconductor is always parallel to the local electrical field. This is commonly expected in an isotropic conductor as the polycrystalline bulk sample investigated in [10]. The current density flowing in the superconductor is then defined using Eq. (10) reported in [9], where the electric field E_c was taken as 10^{-4} V/m. In accordance to [10], the magnetic field dependence of J_c was described by the following equation:

$$J_c(B) = J_{c,0} \exp\left[-\left(\frac{B}{B_0}\right)^{\gamma}\right] \quad (1)$$

where $J_{c,0}$, B_0 and γ are constant parameters.

The magnetic properties of the FM material were defined by the interpolation of the magnetic induction versus applied field curve measured experimentally on small piece of the soft iron used for the shield. The source term for the applied magnetic field, $\mathbf{H_{appl}}$, was considered through the boundary condition: at a large distance from the shield(s), **B** was set at $\mu_0\mathbf{H_{appl}}$. The applied field was always assumed increasing monotonically.

III. CALCULATION RESULTS AND COMPARISON WITH EXPERIMENTAL DATA

Simulations were first performed on a short SC hollow cylinder. Then, they were repeated on the hybrid shield sketched in Fig. 1, consisting of a FM hollow cylinder coaxially mounted outside the SC one. The geometrical parameters of both the cylinders are reported in the caption of Fig. 1. In order to validate the modeling procedure by the comparison with experimental data, the SC shield dimensions and the J_c (B) dependence are the same as for the MgB_2 hollow cylinder studied in [10]. The height difference, Δh, between the edges of the SC/FM cylinders

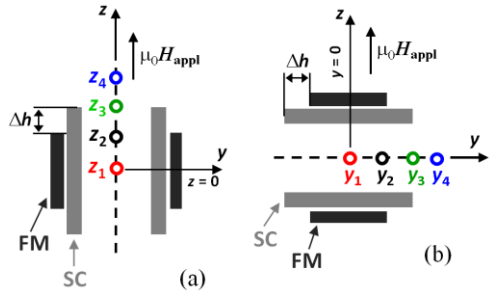

Fig. 1. Schematic view of the SC/FM hollow cylinder arrangement used in the simulations in axial- (a) and transverse- (b) field configuration. Geometrical parameters: SC hollow cylinder: outer radius = 10.15 mm, inner radius = 7.0 mm, height = 17.5 mm; FM hollow cylinder: outer radius = 14.0 mm, inner radius = 11.5 mm, height = 10.5 mm. Δh (= 3.5 mm) represents the height difference between the edges of the SC/FM cylinders. Circles indicate the Hall probe positions in the experiments. Assuming (x,y,z) = (0,0,0) the coordinate of the shield center, in the axial-field configuration the Hall probes were positioned at z_1 = 0 mm, z_2 = 4.4 mm, z_3 = 8.8 mm (SC edge coordinate) and z_4 = 13.1 mm. Likewise, in the transverse-field configuration the Hall probes were placed at y_1 = 0 (shield centre), y_2 = 4.4 mm, y_3 = 8.8 mm (SC edge coordinate), y_4 = 12.0 mm.

was chosen based on previous study outcomes [8],[12] that evidenced how this difference occurrence can improve the magnetic mitigation properties of the hybrid shield.

Fig. 2 compares the induction field curves, B_z, measured in axial-field configuration at T = 30 K by the Hall probes placed along the shield's axis - as shown in Fig. 1(a) - with those calculated in same positions with the procedure described in Sect. II. It is worth mentioning that the Hall probes were always oriented to measure the component of the magnetic induction parallel to $\mathbf{H}_{appl}$ for both the field orientations. Accordingly, the same $\mathbf{B}$ component is plotted in the computed curves. In agreement with [10], to describe the J_c (B) dependence of the superconductor at this temperature, the values $J_{c,0} = 3.01 \times 10^8$ A/m^2, B_0 = 0.83 T and γ = 2.52 were employed in (1). As can be seen, experimental and computed curves are in remarkable agreement both for the SC hollow cylinder alone and the SC/FM arrangement. A good agreement was also found comparing the magnetic induction curves, B_y, measured and

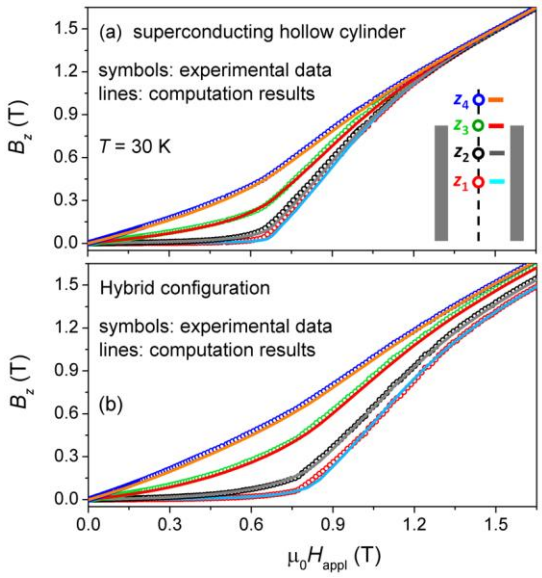

Fig. 2. Comparison between B_z values measured in the axial-field configuration by the Hall probes at T = 30 K and the corresponding curves computed by numerical simulations for the SC hollow cylinder alone (a) and for the hybrid shield (b).

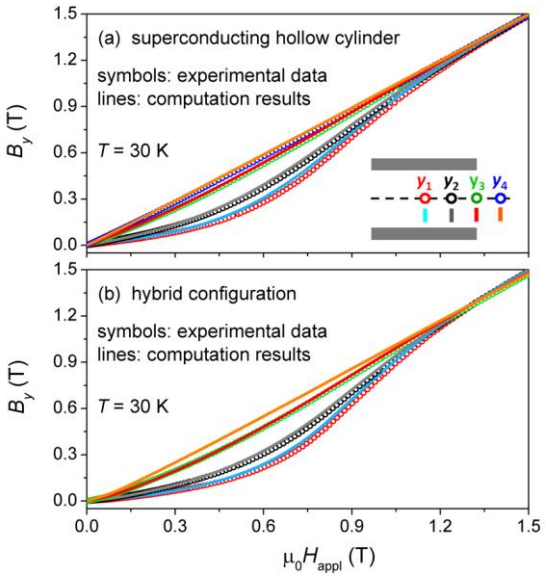

Fig. 3. Comparison between the B_y values measured in the transverse-field configuration by the Hall probes at T = 30 K and the corresponding curves computed by numerical simulations for the SC hollow cylinder alone (a) and for the hybrid shield (b). No experimental data are shown for the hybrid configuration at position y_4 due to a failure of the related Hall probe.

calculated in transverse-field configuration (Fig. 3). Significantly, this measurement-computation agreement is also confirmed at lower and higher temperatures (not shown) validating this modeling approach independently of the use of a specific $J_c(B)$ curve.

These results demonstrate that the chosen modeling procedure is a valuable tool to drive the design of future magnetic shields with a small aspect ratio of height/lateral size but improved shielding performances for various orientations of the applied magnetic field.

ACKNOWLEDGMENT

We wish to thank Fedor Gömöry and Mykola Solovyov for their help in the 3D modeling approach. We are also grateful to Petre Badica and his group that fabricated and provided us the MgB_2 hollow cylinder.

REFERENCES

[1] J. F. Fagnard et al., Supercond. Sci. Technol., vol. 32, Art.no. 074007, July 2019.

[2] Y. Terao et al., IEEE Trans. Appl. Supercond., vol. 21, pp 1584-1587, June 2011.

[3] Ł. Tomków et al., J. Appl. Phys., vol. 117, Art. no. 043901, January 2015.

[4] L. Wéra et al., IEEE Trans. Appl. Supercond., vol. 27, p. 6800305, June 2017.

[5] A. Omura et al., Physica C, vol 386, pp. 506–511, April 2003.

[6] F. Gömöry et al., Science, vol. 335, pp. 1466–1468, March 2012.

[7] L. Gozzelino et al., Supercond. Sci. Technol., vol. 25, p. 115013, November 2012.

[8] L. Gozzelino et al., Supercond. Sci. Technol., vol. 29, Art. no. 034004, March 2016.

[9] M. Solovyov and F. Gömöry, Supercond. Sci. Technol., vol. 32, Art. no. 115001, November 2019.

[10] L. Gozzelino et al., Supercond. Sci. Technol., vol 32, Art. no. 034004, March 2019.

[11] COMSOL Multiphysics® 5.4 software (http://www.comsol.com)

[12] G. P. Lousberg et al., IEEE Trans. Appl. Supercond., vol. 20, pp. 33-41, February 2010.